ELSEVIER

Polymer 42 (2001) 4117–4126

polymer

www.elsevier.nl/locate/polymer

Remnant morphologies in highly-drawn polyethylene after annealing

T. Amornsakchai[a], D.C. Bassett[a,1,*], R.H. Olley[a], A.P. Unwin[b], I.M. Ward[b]

[a]*J.J. Thomson Physical Laboratory, University of Reading, Whiteknights, P.O. Box 220, Reading RG6 6AF, UK*
[b]*IRC in Polymer Science and Technology, University of Leeds, Leeds LS2 9JT, UK*

Received 18 July 2000; received in revised form 2 October 2000; accepted 30 October 2000

Abstract

Specimens of the polyethylene Sclair 2907, full of large banded spherulites, have been drawn to high extensions, and parts of these annealed close to their melting points under constraint. Etching with permanganic reagents and examination under the scanning electron microscope revealed that in transverse sections of the unannealed specimens, the legacy of the banded spherulitic morphology is seen at draw ratio 10× but appears to have been overwritten by subsequent developments at 20× and 33×. However, after annealing, the specimens show recrystallized regions which follow the pattern of the original banded spherulites drawn affinely. This is so even for 33× drawn specimens where the unannealed longitudinal morphology has been overwritten by a new structure of density-deficient regions arranged in parallel bands. It is inferred that different deformation mechanisms operate on bundles of lamellae oriented differently in the original material, and that legacies of the original morphology may be retained at much higher deformations than previously assumed, but they may require appropriate treatments to make them visible.

Keywords: Polyethylene; Remnant morphologies; Deformation

1. Introduction

The characterization of the internal structure of highly oriented fibres is important in the understanding of their mechanical behaviour. In the specific case of fibre strength, the dependence on internal flaws means that a knowledge of the distribution of flaws and their origins is particularly important. In this respect, two significant advances have been made recently.

First, it has been concluded that many highly-drawn advanced polyethylene fibres contain a lateral substructure of density-deficient regions, whose high free volume leads to cratering when transverse cross-sections are exposed to permanganic etchants [1]. This substructure of defects is common to a range of fibres prepared by melt spinning, gel drawing or melt kneading. These flaws are a feature of the fibres as manufactured, but were first seen in compacted materials where the fibres had been taken close to their melting points [2–4]. In consequence, a new model of fibre structure has been proposed which ascribes the density deficiency to these regions having crystallized within a rather rigid framework of the entangled molecular network and so being increasingly under tension as they solidify because of the contraction from the volume of the melt.

Secondly, a recent study of highly oriented polyethylene, drawn at relatively low temperatures from compression moulded sheets, has shown, in contradiction to what was previously believed, that the initial morphology of isotropic material has a significant effect on the internal structure of the drawn material. Surprisingly, it was found that a pronounced legacy of the morphology is retained in the highly-drawn products. This was most obvious in the case of drawing isotropic material containing a banded spherulitic structure where a lateral banded pattern was retained to draw ratios as high as 45 [5]. The banded spherulitic morphology has the particular advantage of inbuilt markers capable of identifying changes occurring during the deformation process and thereby offers the prospect of identifying the origin of texture in the drawn material.

This paper is one of a series in which an isotropic banded spherulitic morphology is used to investigate the development of fibre structure produced by drawing. It reinforces the conclusion of earlier work that a memory of the initial isotropic morphology persists into the drawn material, and shows that although the legacy of the isotropic morphology is obscured by the development of particular types of flaw at

* Corresponding author. Tel.: +44-118-931-8540; fax: +44-118-975-0203.
E-mail address: d.c.bassett@reading.ac.uk (D.C. Bassett).
[1] On leave from the Department of Chemistry, Faculty of Science, Mahidol University, Bangkok 10400, Thailand.

0032-3861/01/$ - see front matter
PII: S0032-3861(00)00815-6

high draw ratio, it re-emerges strongly after constrained annealing to heal these flaws. It also offers an insight into the different types of flaws and their distribution providing a basis for the development of an additional mechanism for flaw formation in drawn samples.

2. Experimental

The material used was the linear polyethylene (LPE) Sclair 2907 produced by Ziegler–Natta catalysis and DuPont, Canada. The average molecular weights are $M_w = 93,600$ and $M_n = 16,800$. Sheets were prepared by compression moulding polymer pellets as supplied at a temperature of 160°C for about 5 min then crystallizing by cooling at a rate of approximately 1 K min^{-1}. Dumbbell specimens (gauge length = 20 mm and width = 5 mm) were cut from these sheets and drawn at 75°C and 100 mm min^{-1} using an Instron tensile testing machine; the draw ratio was calculated from the separation of ink marks printed on the original surface.

To prepare specimens for electron microscopy, both isotropic and drawn materials were embedded in Kraton® G1650 (company under divestment — see www.kraton.-com) block copolymer for ease of handling and microtoming. Their internal surfaces were exposed by removing, at about −70°C in a Bright microtome, longitudinal and preliminary transverse sections with a glass knife, and final transverse sections with a diamond knife. These exposed surfaces were etched, for 1 h at room temperature, with a 1% solution of potassium permanganate in a 10:4:1 (by volume) mixture, respectively, of concentrated sulphuric acid, 85% orthophosphoric acid and water [6]. In addition, in those samples where the original cut surface was required for examination, an RMC ultra-microtome equipped with cryo-chamber set at −120°C and a glass knife were used.

Constrained partial melting was accomplished by embedding a piece of drawn material, approximately 5 mm long, in Araldite™ Rapid in a normal differential scanning calorimeter (DSC) pan. Samples were left for at least 24 h at room temperature to set fully, after which they were heated in the DSC at a heating rate of 10 K min^{-1} to selected temperatures between the onset of melting and its peak, held for 5 s and finally cooled, normally at the setting 160 K min^{-1}. The samples were then embedded in block copolymer and cut transversely and longitudinally as mentioned above. The presence of Araldite™ necessitated two-stage etching of these materials. The first stage used a 1% solution of potassium permanganate in a 5:2:2 (by volume) mixture respectively of concentrated sulphuric acid, 85% orthophosphoric acid and water for 30 min. A final 10 min exposure in a 10:4:1 mixture of the same constituents completed the etching process. A standard two-stage procedure [7] yielded shadowed carbon replicas for TEM studies while for SEM examination, specimen surfaces were examined directly after gold coating.

3. Results

3.1. Pre-annealing morphology

Fig. 1 displays the morphology in transverse and longitudinal directions of Sclair 2907 drawn to draw ratios of 10×, 20× and 33×. It is apparent that different regions of the material have different resistance to the permanganic etchant especially in the transverse direction, where cratering develops. Following studies on highly-drawn polyethylene fibres prepared by processes as different as melt spinning, gel drawing and melt kneading [1], it was established that those areas where etchant is most penetrable are density-deficient and develop under etchant attack to give conical craters such as those seen here in transverse section. In the 10× (Fig. 1a) specimen it can be seen that the craters form a regular pattern as a result of the banded spherulitic structure in the original isotropic material. Often many craters are aligned so close together that they merge to form concentric furrows, whose spacing in the deformed sample corresponds to affine deformation of the original banded spherulitic pattern, the scale of which is indicated in the bar at the top of the picture. In the 20× (Fig. 1b) specimen, the craters are larger and the furrows are bigger than at 10×, whereas they would be expected to be smaller for affine deformation, as indicated by the bar. A change in transverse morphology is seen in the 33× sample (Fig. 1c) in which the surface is covered in deeply etched bands which, at the centre, also seem to display something of the concentric banded morphology, but here again the scale exceeds that expected for affine deformation. This differs from results reported previously [5] on a metallocene polyethylene in which the affine relation held to 20× and in parts of the specimen to 35× draw.

The longitudinal morphology is visibly oriented with a fine pattern in the first two samples, though it is particularly bland at 10× (Fig. 1d) but a little more prominent at 20× (Fig. 1e). However, a dramatic change in longitudinal morphology is seen in the 33× sample (Fig. 1f) in which a large number of parallel longitudinal etched pockets are laid in the regions between almost parallel continuous transverse bands. This has been encountered previously in polypropylene (PP) [8] and is a consequence of alternating zones of different draw ratios within a uniform cross-section. The two different ratios for alternate zones in series impose lateral tensions on the more highly-drawn ones resulting in transverse crazing or density-deficient regions. Etching develops these into laterally alternating fibres and voids; the entire bands are unaffected. This structure has been referred to as a 'Pisa' structure from its resemblance to the facade of the Leaning Tower [5]. On etching of transverse sections, it was found that in the PP [8] and the metallocene polyethylene PF3 [5], smooth and deeply pitted regions were observed, the deeply pitted ones where the etched surface passed through the density-deficient bands and the smooth regions corresponding to the entire bands

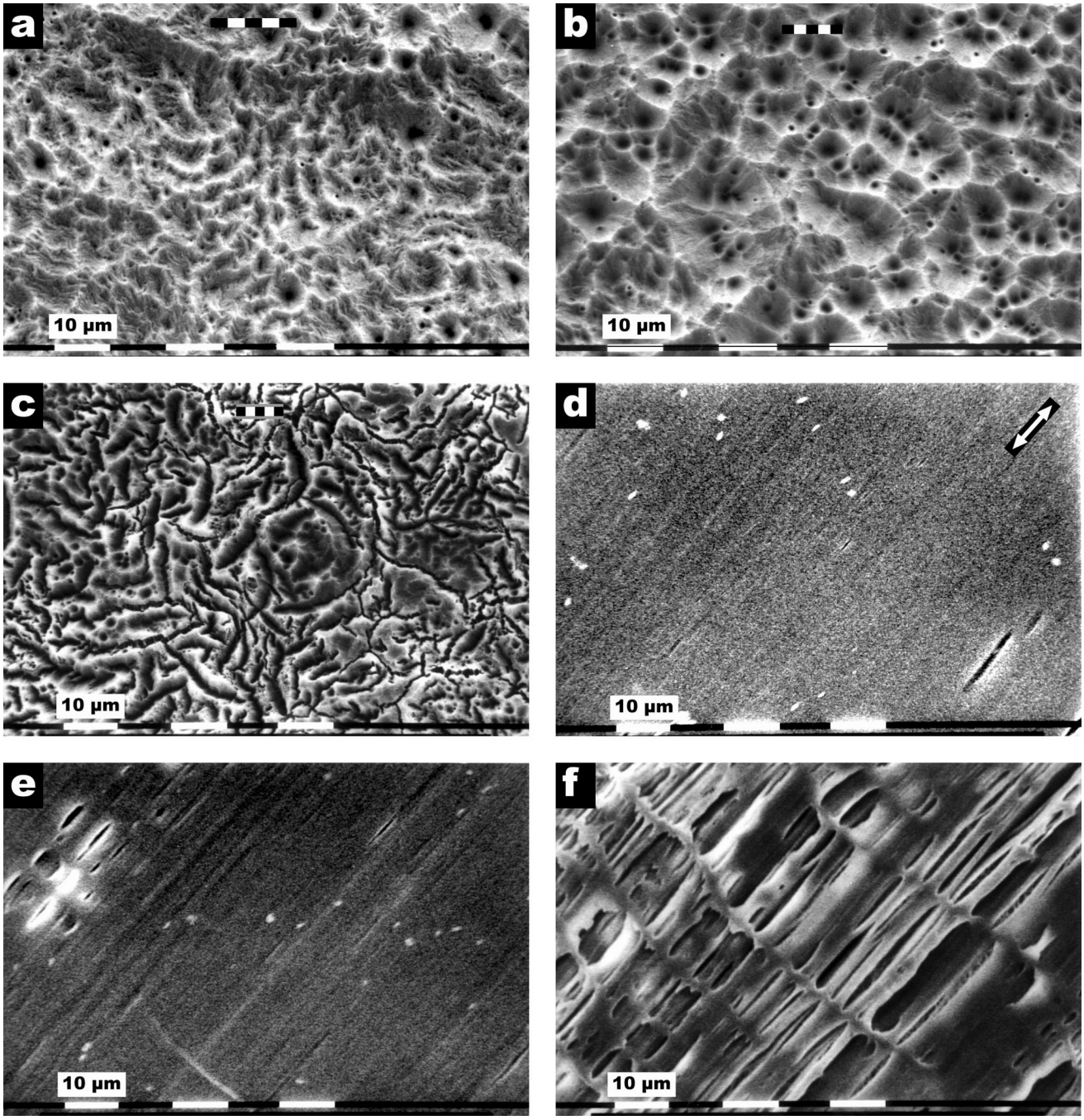

Fig. 1. SEM of transverse (a–c) and longitudinal morphologies (d–f) of Sclair 2907 drawn to draw ratios of 10 × (a, d), 20 × (b, e) and 33 × (c, f). Striped bars at top of a, b and c show the band period calculated for affine deformation. Draw direction in longitudinal specimens as arrowed on 1d.

which proved resistant to downward etching, like 'mesas' in the North American desert. The transverse bands in the present structures are more heavily indented than those seen earlier in the metallocene polyethylene PF3 [5], which would mean that they are more easily attacked and do not survive to produce significant areas of 'mesa' structure. In the metallocene polyethylene, in some of the porous areas in the 'mesa' structure, it appeared that the affine relation held to 35 ×, showing local evidences of concentric banding with the appropriate period.

Fig. 2 shows SEM micrographs of a cryogenically cut surface of this sample, prepared to check the association of the voids in the etched sample with density-deficient regions in the untreated sample. The specimen appeared largely solid, but also displayed slight longitudinal depressions and occasional longitudinal craze-filled cracks, corresponding to the longitudinal voids opened up by the etchant. Knife marks can also be seen running diagonally, which helps to ensure that the features seen are genuine and not knife-generated. As already observed in compacted

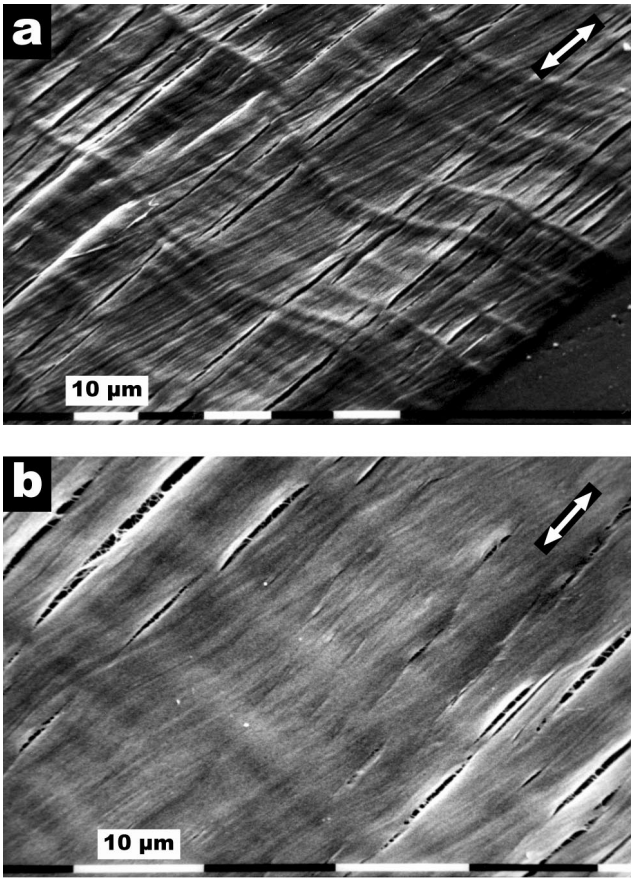

Fig. 2. (a) Tilted and (b) flat-on SEM of cryogenically cut longitudinal surface of Sclair 2907 drawn to a draw ratio of 33×. Longitudinal draw directions as arrowed.

specimens [2], cut surfaces often show relaxation features which are closely related to the underlying morphology. In the present case it was not necessary to develop these features by solvent treatment [9], since the surfaces as cut, revealed the transverse banding in slight relief.

3.2. Thermal treatment and analysis

Before performing selective melting experiments it is necessary to obtain DSC thermograms of the constrained samples. Fig. 3 shows these melting traces for epoxy-embedded 10×, 20× and 33× drawn samples. As the material displays structural inhomogeneities, especially at a draw ratio of 33×, it might be expected to show inhomogeneities, in its thermal stability, possibly leading to a bimodal trace in DSC [10]. In practice, however, all traces show only one sharp peak. Constraint was found to shift the melting onset and peak temperatures from the unconstrained samples (data not shown) upwards by about 1°C at all three draw ratios. This is in contrast to what has been found for fibres prepared by gel drawing or melt kneading where the shift was in the order of some 10°C [11]. For each sample, three temperatures were chosen for partial melting experiments. The temperature midway between the onset

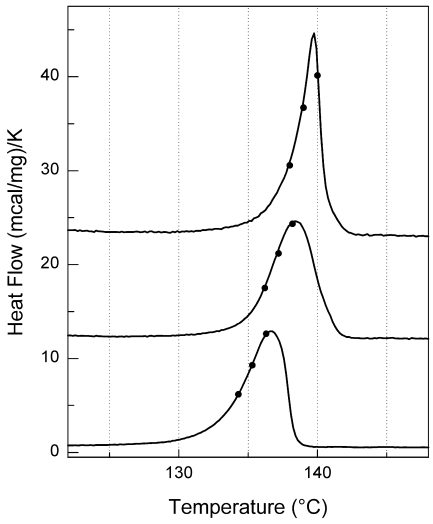

Fig. 3. DSC traces of epoxy-embedded drawn Sclair 2907 of draw ratios 10× (bottom), 20× (middle) and 33× (top). The solid circles on each trace are temperatures at which partial melting of each sample was carried out.

and melting peak was chosen as the middle set temperature in each range, although in practice the DSC settled asymptotically to a temperature 0.7°C higher than this over a period of 5 s, according to the difference between the calibrations of the instrument for the dynamic (10 K min^{-1}) and static conditions. The two remaining annealing temperatures were positioned ±1°C relative to this, as shown by the solid circles representing the actual attained temperatures in Fig. 3.

3.3. Annealed morphology: SEM observations

The progressive changes in morphology with annealing are very similar in the 10× (Fig. 4) and the 20× (Fig. 5) materials. The cratered morphologies observed in the original transverse sections are all completely transformed, passing through various stages as the annealing temperature is increased. The earliest stages of transformation are seen in the 10× drawn material (Fig. 4a–c). Even at the lowest temperature (Fig. 4a) the crater structure in the original material (Fig. 1a) has completely disappeared, being replaced by a lamellar morphology with a somewhat 'zigzag' appearance which can just be made out as following a ring pattern on the same scale as the unannealed morphology. The ring pattern becomes more pronounced as the annealing temperature increases, and at the highest temperature the onset of contrast between two types of morphology appearing light and dark is quite discernible. A somewhat similar development is seen for the 20× drawn material (Fig. 5a–c), although there are two features which should be noted. First, the development of alternating morphology at the highest temperature is much more pronounced. This may relate in part to the different draw ratios, but in addition the sample has been annealed closer to

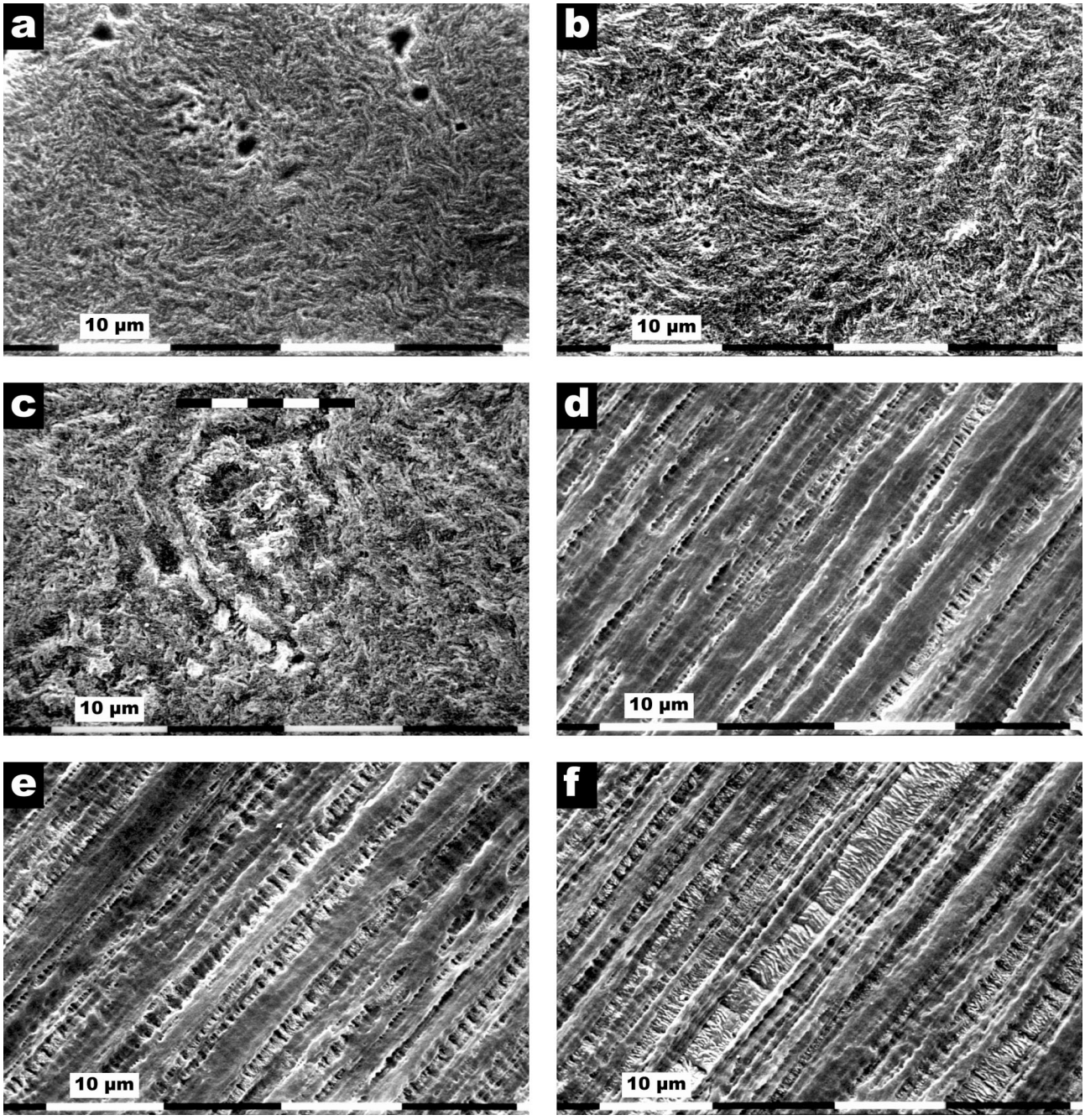

Fig. 4. SEM of transverse (a–c) and longitudinal morphologies (d–f) of Sclair 2907 drawn to a draw ratio of 10× and partially melted at 134.3°C (a, d), 135.3°C (b, e), and 136.3°C (c, f). Bar at top of (c) indicates the expected 'recovered' band period. Longitudinal draw direction as arrowed on 1d.

its final melting point, as a result of the original melting peak being narrower, and this factor may well be the more important. Secondly, the periodicity is altered by annealing to one corresponding more closely with affine deformation of the banded texture.

Two changes in the longitudinal morphology with annealing temperature are apparent. At the lower and middle annealing temperatures for both 10× and 20× materials (Figs. 4 and 5, d and e) the generally lightly marked texture of the unannealed materials has become rather more rugged, and in addition there are long pockets opened out by the etchant, which have been filled with stacks of lamellae with their *c*-axes parallel to the draw direction. At the higher temperature (Figs. 4f and 5f) the pockets become continuous bands filled with lamellae. These features are similar to the infilling lamellae in compacted PE, which serve as the binder in that process [2]. Their quantity and distribution suggest that these constitute the darker areas in the concentric ring structures seen in the corresponding transverse sections (Figs. 4c and 5c).

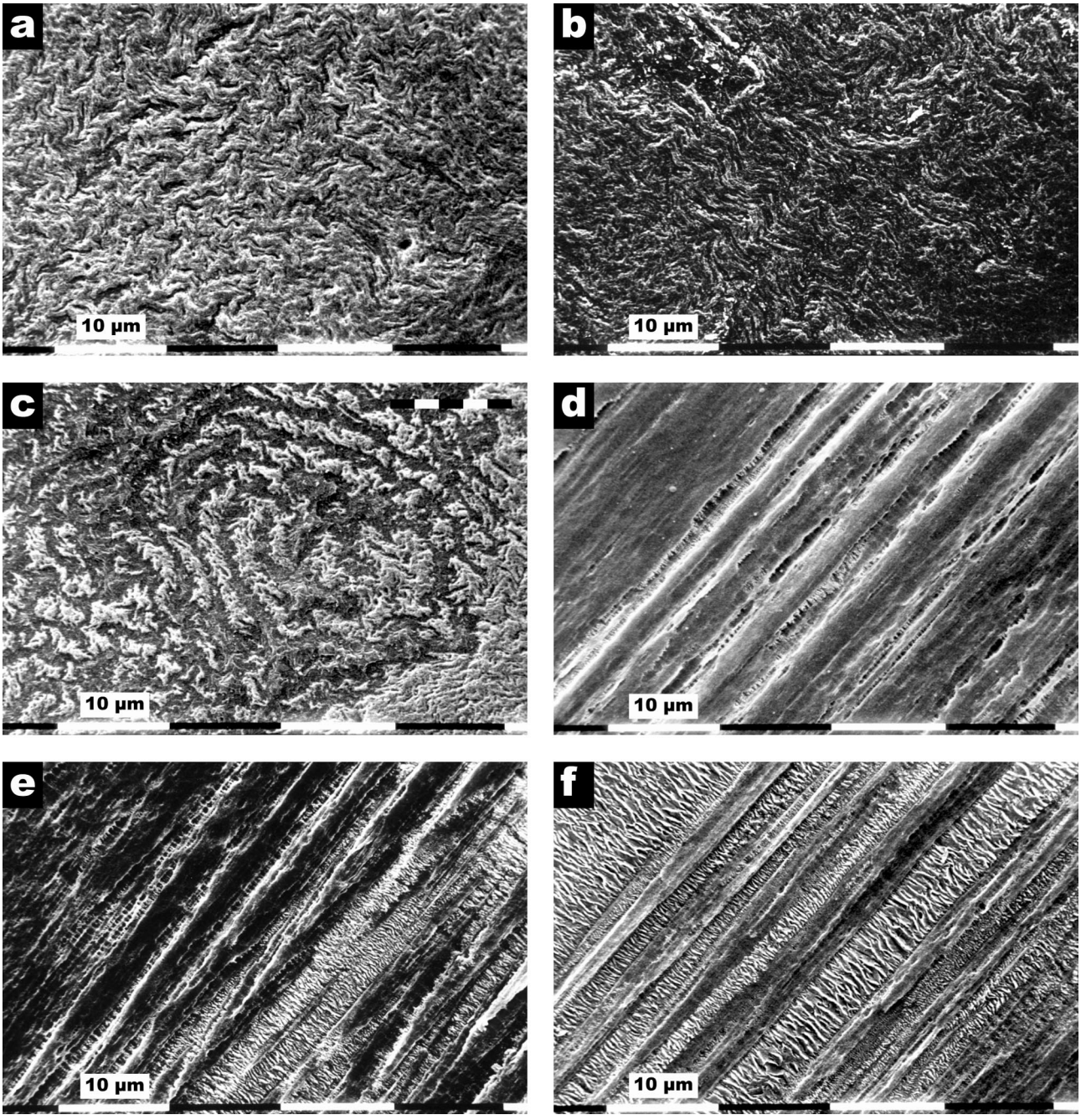

Fig. 5. SEM of transverse (a–c) and longitudinal morphologies (d–f) of Sclair 2907 drawn to a draw ratio of 20 × and partially melted at 136.2°C (a, d), 137.2°C (b, e), and 138.2°C (c, f). Bar at top of (c) indicates the expected 'recovered' band period. Longitudinal draw direction as arrowed on 1d.

The progress of annealing is rather different in the 33 × material (Fig. 6). While some of the differences are due to the narrowness of the melting peak and greater degree of conversion of the solid to melt, even at the lowest temperature the morphology is rather different from the previous two materials, revealing large crevices from the density-deficient regions, which as the corresponding longitudinal section will show (Fig. 6d), have resulted from the coalescence of the 'craze-like' structures present in the unannealed specimen (Fig. 1f). However, the smaller craters found in the original (Fig. 1c) have disappeared, and the banding has become much more prominent. By the middle temperature (Fig. 6b) the deeply etched bands have largely been healed in certain regions where the concentric banded structure has been transformed to a similar alternating appearance to that which was beginning to appear at the higher temperatures in the lower draw ratio materials. At the highest temperature, most of the material has melted with only a small fraction still remaining solid on which the large areas of melt have nucleated upon cooling. The

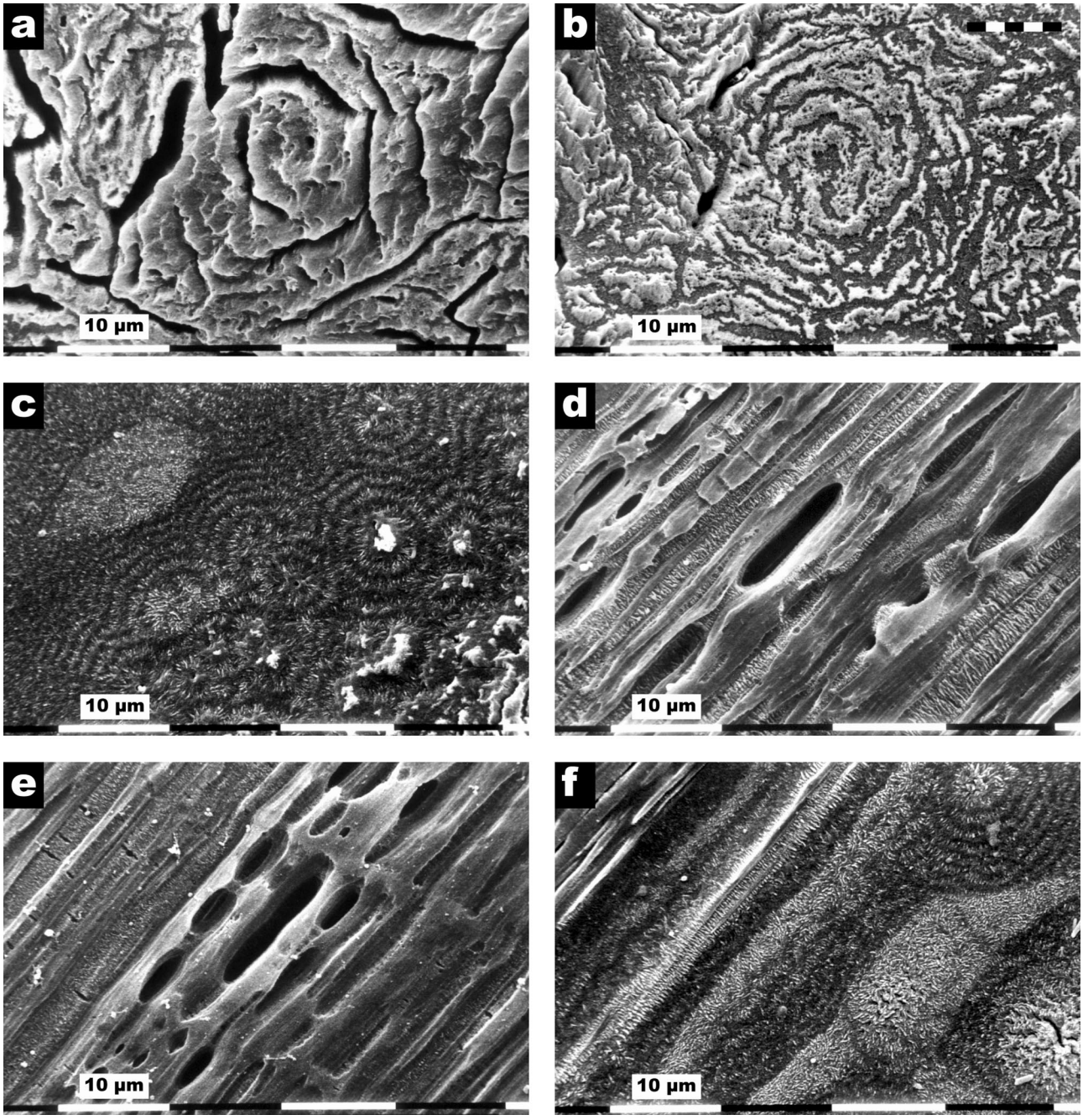

Fig. 6. SEM of transverse (a–c) and longitudinal morphologies (d–f) of Sclair 2907 drawn to draw ratio of 33 × and partially melted at 138.0°C (a, d), 139.0°C (b, e), and 140.0°C (c, f). Bar at top of (b) indicates the expected 'recovered' band period. Longitudinal draw direction as arrowed on 1d.

morphology found in the recrystallized melt is normal banded spherulitic structure, but on a finer scale than in the original, a consequence of the cooling applied in the DSC being much faster than in the preparation of the original sheet.

The longitudinal sections are also seen to have undergone drastic modification. At the lower and middle temperatures (Fig. 6d and e) the 'Pisa' structure has been transformed almost beyond recognition in that the density-deficit no longer appears as a mass of fine bands, but has coalesced in regions with much more coherent material between them. Nevertheless, even at the middle temperature (Fig. 6e) traces of the transverse banding are still apparent. Long pockets of stacked lamellae have appeared as at the lower draw ratios. Particularly, considering Fig. 6b, it is apparent that the 'Pisa' structure, which appeared to have overwritten the memory of the original spherulitic banding, has not in fact destroyed the legacy of the banding which has reappeared under the appropriate annealing conditions. At the highest temperature (Fig. 6f), the structure is practically

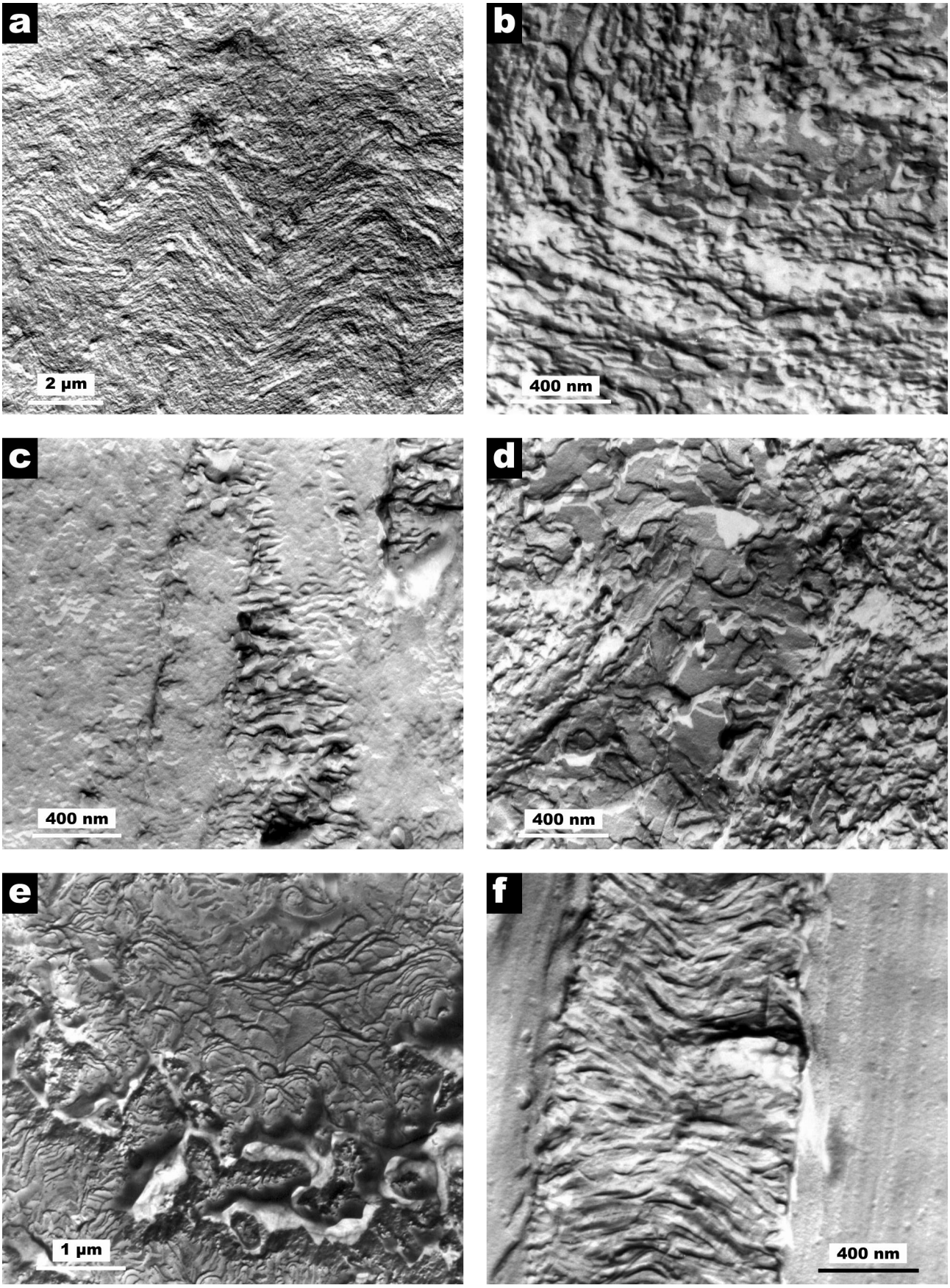
a
2 μm
b
400 nm
c
400 nm
d
400 nm
e
1 μm
f
400 nm

completely transformed as understood from the transverse section (Fig. 6c), but the linearity of the solid remnants is to be noted.

Measurements of the band spacing are complicated by the different perspectives that the structures can present when sections through the bulk material are taken. A detailed quantitative analysis was not considered appropriate here but considerable effort was made to verify the reproducibility of the results. Accordingly, the conclusions are semi-quantitative but sufficiently reproducible to support the general conclusions reached. In summary, it is found that for all three drawn samples the banding that develops with annealing is affinely related to that of the isotropic material, even though in the more highly-drawn samples, the band spacing in the unannealed material, as revealed after etching, had deviated considerably from affine.

3.4. TEM observations

Results of detailed investigation of the morphology by replication and TEM of the 10× sample which was partly melted at 135.3°C are shown in Fig. 7a and b. These show, at medium and high magnification, respectively, the zigzag regions found in the transverse direction. This two-dimensional zigzag pattern corresponds in periodicity to the series of alternating ridges and furrows in the unannealed specimen. It is difficult, however, to discern the precise relative relief of the different components of this structure. From Fig. 7b it can be seen that the building blocks of this feature are in fact small flat-on lamellae stacked on top of one another and that the etchant has penetrated these in a zigzag pattern. It is, however, difficult to conceive at this stage how the pattern originates structurally. The longitudinal section (Fig. 7c) shows more clearly how the material is beginning to differentiate into two parts, of which the greater part is composed of fine lamellar blocks while the lesser part has melted and recrystallized, giving lamellae with greater lateral extent, and with enough amorphous material between them to be etched out into grooves, giving the observed greater contrast. A similar process may be responsible for the development of greater contrast to reveal the lamellar blocks in those regions where melting and recrystallization have not occurred. In this respect, it is to be noted that these lamellar blocks are dimensionally similar to what might be expected from typical long period measurements [12]. The 20× material, annealed at 137.2°C, shows the melting and recrystallization process taken further, so that in transverse section (Fig. 7d) there are now distinct bands of wider lamellae, which would appear darker under SEM.

The ringed structure displayed in the 33× material after annealing at the middle temperature (Fig. 7e) appears to be similarly composed of even wider lamellae (which would appear dark under the SEM) and regions of much finer texture. The latter regions, which stand proud in the specimen and appear bright under SEM, are so rugged that the corresponding grooves or pits in the replica are hidden from the shadowing metal, so that their structure is in many places obscure. This confirms the impression of a 'ridge and furrow' structure seen in Fig. 6b, and by implication in Fig. 5c. In a longitudinal section (Fig. 7f) the contrast between unmelted and recrystallized regions is similar to that for lower draw ratios. The way in which the lamellae have regrown in the melt from the walls of unmelted material is evident.

4. Discussion

The present work shows conclusively that drawn material retains a memory of the initial morphology. This reinforces conclusions already reached following studies of a range of polyethylenes [5], but the existence in the drawn material of a periodic thermal stability linked to the inbuilt markers provided by the banded spherulite and the clearer emergence of texture with annealing show that this persists to much higher draw ratios than previously shown.

It is envisaged that this memory is provided through a deforming network which underpins the microstructure and which has already been identified [13,14] as a key factor in the deformation process. The retention of a memory indicates that, despite necking and inhomogeneous macroscopic deformation, the post neck structure is related to the original. The dimensions indicate that on a macroscopic scale, the deformation is close to affine, even though at the scale of the banding, local non-affine deformation must occur. This is necessarily so at the lamellar level where the local *c*-axis orientation in particular will have a bearing on which deformation modes are operative [15].

The course of deformation is such that at 10× an apparently fully oriented structure has formed. While there are no variations visible in longitudinal section (Fig. 1d) which could be readily related to the starting morphology, the lateral variations in porosity, which in transverse section are developed on etching into the cavities seen as Fig. 1a, do show the continuity with the original banded morphology. These must be a consequence of differential deformation deriving from the initial variation in molecular and lamellar orientation within the spherulites. In the previously studied metallocene material [5], this continuity could be followed through to higher draw ratios, but in the present Ziegler–Natta polymer, the porosity becomes coarser with increasing draw, rather than finer as would happen if it were to follow the dimensions of the banding under affine deformation.

Fig. 7. TEM of drawn Sclair 2907 specimens treated at the respective middle annealing temperatures: transverse (a, b) and longitudinal (c) morphologies of 10× drawn (d) transverse morphology of 20× drawn and transverse (e) and longitudinal (f) morphologies of 33× drawn materials.

At higher draw ratios, a different form of porosity develops, which is responsible for the bands ('Pisa' structure) in longitudinal sections (Fig. 1f). In transverse section the corresponding structure, with deeply etched bands, comes to be superposed on the spherulitic banding and provides the dominant contrast, in the Sclair to a much greater extent than in the metallocene polyethylene [5]. However, although the original banded structure is lost to sight, a banded texture of affine dimensions reappears on annealing. Figs. 5c and 6b display the 'ridge and furrow' etched structure expected if there was a pattern of density-deficient regions which followed the initial morphology, but this is not the case in the unannealed material. It is, therefore, more likely that the density deficiencies formed after annealing, which allow access of etchant, are in the form of screw dislocations as are commonly found in parallel stacks of lamellae, and are thus a product of the recrystallization process. The occurrence of patterns as in Figs. 5c and 6b is a striking demonstration of the memory of the entangled molecular network. At 20× this can no longer be laterally uniform — otherwise the original banding would still be revealed in the etched unannealed specimens — but even at 33× it must survive to some extent in order to give the 'concentric' appearance seen in Fig. 1c. Once the structure has become sufficiently mobile to heal the local deformation that gave rise to the 'Pisa' structure, banding is able to re-establish itself as the dominant factor in producing the observed morphology.

The differing internal thermal stability when drawn samples are annealed indicates differences in respect either of crystallite size or crystallite perfection in the drawn regions. The periodic nature of this phenomenon is strongly suggestive of different deformation mechanisms operating according to differing initial lamellar orientations. These phenomena would accordingly be expected to develop systematically throughout spherulites. It has previously been shown [16] that, at a low draw ratio, deformation of spherulites leads to disruption particularly along the major axes and a consequent lower melting stability. The present work has since been extended to the study of developing textures at low draw ratios, to be published elsewhere.

Differing local deformation mechanisms will also affect the network structure. One notable feature which these SEM and TEM observations have brought out is that, while the unannealed morphology with its craters developed by permanganic etching bears a striking resemblance to that of melt-spun fibres [1] the progress of melting here follows different courses. In the melt-spun fibres, internal melting starts specifically at the density-deficient regions, where there is more free volume for molecules to move. In the partly melted and recrystallized fibres the partly molten structure is retained to the extent that the lamellae which form in the melted regions are found at the bottom of craters after etching [17]. In the present case, crater structures do not form even at the lowest annealing temperatures. Differential melting here is most likely dominated by differences in crystal perfection.

A final corollary of this work, which has demonstrated variation in the lateral scale of an inferred molecular network following the original morphology, is that such variation is a credible potential cause of variations in properties of other highly extended polyethylenes and other oriented polymers.

5. Conclusions

The current work provides further unequivocal evidence for the retention of a morphological memory in drawn samples and underlines the significance of the molecular network underpinning the morphology. In particular, this memory of the undeformed morphology can be amplified by partial melting. This is most evident in transverse sections where the banding is found first to become less distinct with draw ratios then to re-emerge strongly following partial melting, with periodicity scaled as for affine deformation of the undrawn banded morphology. It is inferred that areas of differing thermal stability in the drawn material are related to differing local lamellar orientations in the starting material, and consequently, to different deformation mechanisms operating thereon. Partial melting and recrystallization further identifies lateral differences in the internal structure of highly-drawn polyethylene.

References

[1] Abo El Maaty MI, Olley RH, Bassett DC. J Mater Sci 1999;34:1975.
[2] Olley RH, Bassett DC, Hine PJ, Ward IM. J Mater Sci 1993;28:1107.
[3] Kabeel MA, Bassett DC, Olley RH, Hine PJ, Ward IM. J Mater Sci 1994;29:4694.
[4] Yan RJ, Hine PJ, Ward IM, Olley RH, Bassett DC. J Mater Sci 1997;32:4821.
[5] Amornsakchai T, Olley RH, Bassett DC, Al-Hussein M, Unwin AP, Ward IM. Polymer 2001;41:8291.
[6] Shahin MM, Olley RH, Blissett MJ. J Polym Sci Polym Phys Ed 1999;37:2279.
[7] Willison JHM, Rowe AJ. Replica, shadowing and freeze-etching techniques. Amsterdam: North Holland, 1980.
[8] Abo El Maaty MI, Bassett DC, Olley RH, Dobb MG, Tomka JG, Wang IC. Polymer 1996;37:213.
[9] Bartosiewicz I, Mencik Z. J Polym Sci Polym Phys Ed 1974;12:1163.
[10] Bassett DC. Principles of polymer morphology. Cambridge, UK: Cambridge University Press, 1981.
[11] Teckoe J, Bassett DC., Olley RH. Polym J. 1999;31:765.
[12] Corneliussen R, Peterlin A. Makromol Chem 1967;105:193.
[13] Capaccio G, Crompton TA, Ward IM. J Polym Sci Polym Phys Ed 1976;14:1641.
[14] Capaccio G, Ward IM. Colloid Polym Sci 1982;260:46.
[15] Lee SY, Bassett DC, Olley RH. J Mater Sci 2001;35:5101.
[16] Bassett DC, Freedman AM. Prog Colloid Polym Sci 1993;92:23.
[17] Kabeel MA, Bassett DC, Olley RH, Hine PJ, Ward IM. J Mater Sci 1995;30:601.